

# Lipid phosphate phosphatase-1 expression in cancer cells attenuates tumor growth and metastasis in mice<sup>S</sup>

Xiaoyun Tang,\* Matthew G. K. Benesch,\* Jay Dewald,\* Yuan Y. Zhao,† Neeraj Patwardhan,§ Webster L. Santos,§ Jonathan M. Curtis,† Todd P. W. McMullen,\*\* and David N. Brindley<sup>1,\*</sup>

Signal Transduction Research Group, Department of Biochemistry,\* University of Alberta, Edmonton, Alberta, T6G 2S2, Canada; Department of Agricultural, Food and Nutritional Science,† University of Alberta, Edmonton, Alberta T6G 2P5, Canada; Department of Chemistry,§ Virginia Tech, Blacksburg, VA 24061; and Department of Surgery,\*\* University of Alberta, Edmonton, Alberta, T6G 2R7, Canada

**Abstract** Lipid phosphate phosphatase-1 (LPP1) degrades lysophosphatidate (LPA) and attenuates receptor-mediated signaling. LPP1 expression is low in many cancer cells and tumors compared with normal tissues. It was hypothesized from studies with cultured cells that increasing LPP1 activity would decrease tumor growth and metastasis. This hypothesis has never been tested in vivo. To do this, we inducibly expressed LPP1 or a catalytically inactive mutant in cancer cells. Expressing active LPP1 increased extracellular LPA degradation by 5-fold. It also decreased the stimulation of  $Ca^{2+}$  transients by LPA, a nondephosphorylatable LPA<sub>1/2</sub> receptor agonist and a protease-activated receptor-1 peptide. The latter results demonstrate that LPP1 has effects downstream of receptor activation. Decreased  $Ca^{2+}$  mobilization and Rho activation contributed to the effects of LPP1 in attenuating the LPA-induced migration of MDA-MB-231 breast cancer cells and their growth in 3D culture. Increasing LPP1 expression in breast and thyroid cancer cells decreased tumor growth and the metastasis by up to 80% compared with expression of inactive LPP1 or green fluorescent protein in syngeneic and xenograft mouse models.▣ The present work demonstrates for the first time that increasing the LPP1 activity in three lines of aggressive cancer cells decreases their abilities to produce tumors and metastases in mice.—Tang, X., M. G. K. Benesch, J. Dewald, Y. Y. Zhao, N. Patwardhan, W. L. Santos, J. M. Curtis, T. P. W. McMullen, and D. N. Brindley. **Lipid phosphate phosphatase-1 expression in cancer cells attenuates tumor growth and metastasis in mice.** *J. Lipid Res.* 2014. 55: 2389–2400.

**Supplementary key words** autotaxin • breast cancer • thyroid cancer • cell migration • epidermal growth factor receptor • G-protein-coupled receptors • lysophosphatidate

The bioactive lipid lysophosphatidate (LPA) is produced mainly by the secreted enzyme autotaxin (ATX) (1–3). The ATX gene is among the 40 most upregulated genes in metastatic cancers (4). LPA signals through at least six G-protein-coupled receptors to increase cell division, survival, migration, and angiogenesis (1–3). Overexpression of ATX, LPA<sub>1</sub>, LPA<sub>2</sub>, or LPA<sub>3</sub> receptors in mammary cells causes spontaneous development of mammary tumors in mice (5). Women with breast carcinomas that express high levels of LPA<sub>3</sub> receptors in cancer epithelial cells, or ATX in stromal cells, have larger tumors, nodal involvement, and higher stage disease (6). LPA produces resistance to the cytotoxic effects of paclitaxel (2, 7–9), carboplatin (10), and radiation-induced cell death (2, 11, 12). Inhibiting ATX activity and lowering LPA concentrations in plasma and tumors decreases the initial phase of breast tumor growth and subsequent lung metastasis by ~60% in a mouse model (13). These combined results provide strong evidence that increased LPA signaling in cancer cells promotes the growth and metastasis of breast tumors.

The present studies focus on a different approach to attenuating LPA signaling. This involves increasing the expression of lipid phosphate phosphatase-1 (LPP1), which is a member of a family of three phosphatases that dephosphorylate bioactive lipid phosphates and pyrophosphates (14–16). Despite this broad specificity for lipid phosphates that is observed with cell-free systems, changing the expression of the different LPPs in animal models produces different

Abbreviations: ATX, autotaxin; BAPTA, 1,2-bis(o-aminophenoxy) ethane-*N,N,N,N*-tetraacetic acid; EGF, epidermal growth factor; FBSC, charcoal-stripped FBS; FLAG, an octapeptide tag consisting of AspTyr-LysAspAspAspAspLys; GFP, green fluorescent protein; LPA, lysophosphatidate; LPP, lipid phosphate phosphatase; PAR1, protease-activated receptor-1; PI3K, phosphatidylinositol 3-kinase; PDGF, platelet-derived growth factor; PLC, phospholipase C; PLD, phospholipase D; PTX, pertussis toxin; S1P, sphingosine 1-phosphate; SCID, severe combined immunodeficiency.

<sup>1</sup>To whom correspondence should be addressed.

e-mail: david.brindley@ualberta.ca

▣ The online version of this article (available at <http://www.jlr.org>) contains supplementary data in the form of five figures.

T.P.W.M. was supported by the Canadian Institutes of Health Research (CIHR). D.N.B. was supported by grants from Canadian Breast Cancer Foundation (CBCF), Women and Children's Health Research Institute of the University of Alberta, and CIHR with the Alberta Cancer Foundation. X.T. holds a research fellowship from the CBCF. M.G.K.B. received a Vanier Canada Graduate Scholarship from the Government of Canada, a Killam Trust Award, and an MD/PhD scholarship from Alberta Innovates-Health Solutions.

Manuscript received 29 July 2014 and in revised form 8 September 2014.

Published, JLR Papers in Press, September 10, 2014

DOI 10.1194/jlr.M053462

phenotypes. This demonstrates that the different LPPs have separate and nonredundant functions in vivo (14, 16).

LPP1 is partially expressed on plasma membranes, and this ecto-activity degrades extracellular LPA (17–19). Knockdown of LPP1 in mice increases circulating LPA concentrations and prolongs the half-life of plasma LPA from 3 to 12 min (18). LPP1 also attenuates signaling downstream of G-protein-coupled receptors and receptor tyrosine kinases. This effect depends on the catalytic activity of LPP1 and presumably results from the degradation of an intracellular lipid phosphate(s) formed downstream of receptor activation (14, 15, 20, 21). These combined actions are consistent with reports that increasing LPP1 activity in cells suppresses signals that promote cell growth and migration (2, 15, 16). Work with the *Drosophila* LPPs, Wunen and Wunen-2, confirms a role in controlling the survival and migration of germ cells. In addition, the Wunen proteins serve an essential tissue-autonomous role in development of the trachea and in the integrity of the blood-brain barrier (22).

These latter properties of LPP1 (3) are significant in terms of cancer biology because total LPP activity is low in many tumors (23–25). This results in increased LPA concentrations in ascites fluid of ovarian cancer patients (25). Microarrays from the Oncomine™ database show that LPP1 expression is decreased in human breast, ovarian, melanoma, colorectal, renal, and lung cancers and in leukemias compared with normal control tissue (supplementary Fig. 1). Gonadotropin-releasing hormone increases ecto-LPP expression, and this decreases the proliferation of ovarian cancer cells (24). Increased expression of LPP3 increases the degradation of extracellular LPA, and this decreases the growth of ovarian cancer cells and colony formation. It was hypothesized from work in vitro that increasing LPP3 expression could provide a novel therapy strategy for cancer (25, 26).

Despite this evidence for a potential role for the LPPs in controlling the phenotype of cancer cells in culture, there is no present proof that increasing LPP1 or LPP3 activity in cancer cells can decrease tumor growth and metastasis in animals. We, therefore, studied the effects of increasing the low expression of LPP1 in human and mouse breast cancer cells on their response to growth factors in vitro and their ability to form tumors and metastases in mice. As controls we expressed a catalytically inactive mutant, LPP1(R217K), or green fluorescent protein (GFP). Increasing the catalytic activity of LPP1 in breast cancer cells decreased the LPA-induced activation of RhoA and Ca<sup>2+</sup> transients. LPP1 expression also decreased Ca<sup>2+</sup> transients produced by a nondephosphorylatable LPA<sub>1/2</sub> receptor agonist and by protease-activated receptors. This demonstrates that this LPP1 effect cannot be explained by its ecto-phosphatase activity. LPP1 expression also decreased the division of breast cancer cells in 3D culture and their ability to migrate in response to LPA. Inducible expression of active LPP1 decreased tumor growth and lung metastasis by up to 80% in syngeneic and xenograft mouse models of cancer. These effects were observed in the absence of significant changes in the concentrations of LPA in the

tumors or plasma of the mice. This work demonstrates for the first time that increasing LPP1 in three lines of aggressive cancer cells decreases their ability to form tumors and metastases in vivo. This work with mouse models is an essential component in understanding the biological functions of LPP1 and translating this knowledge into the prevention of tumor progression.

## MATERIALS AND METHODS

### Reagents

Oleoyl-LPA (233019) and *D-erythro*-S1P (860492) were from Avanti Polar Lipids (Alabaster, AL). Wls-31 was synthesized as described previously (27). Protease-activated receptor-1 (PAR1) peptide was a gift from Dr. M. Hollenburg (University of Calgary, Alberta, Canada). Other reagents were purchased as follows: epidermal growth factor (EGF) (CRE009B) (Cell Sciences, Canton, MA); doxycycline (0219895525) (MP Biomedicals, Solon, OH); mouse anti-phospho-Akt (4051S), rabbit anti-Akt (4691S), mouse anti-phospho-ERK (9106S), rabbit anti-ERK (9102S), and rabbit anti-Ki67 (12202S) antibodies (Cell Signaling Technologies, Danvers, MA); rabbit anti-CD31 (ab28364) antibody (Abcam, Toronto, Ontario, Canada); mouse anti-FLAG (F1804) antibody to the octapeptide, AspTyrLysAspAspAspLys, fatty acid-free BSA (A8806), 1,2-bis(o-aminophenoxy)ethane-*N,N,N,N*-tetraacetic acid (BAPTA)-AM (A1076), LY294002 (L9908), U73122 (U6756), U73343 (U6881), wortmannin (W1628), pertussis toxin (PTX) (P140), and probenecid (P8761) (Sigma, St. Louis, MO); PolyJet (SL100688) (SignaGen Laboratory, Gaithersburg, MD); G418 sulfate (11811-031), LR clonease enzyme mix (11791-019), Fura-2 AM (F-1201), and F127 (P-6867) (Life Technologies, Grand Island, NY); PfuUltra DNA polymerase (600385) (Agilent Technologies, Santa Clara, CA); restriction enzymes *SpeI* (R0133), *SalI* (R0138), *XhoI* (R0146), and T4 DNA ligase (M0202) (New England Biolabs, Ipswich, MA); Matrigel (354230/354234) (BD Biosciences, San Jose, CA); terminal deoxynucleotidyl transferase dUTP nick end labeling (TUNEL) assay kit (APT110) (Millipore, Billerica, MA); and RhoA (BK036), Rac (BK035), and cdc42 (BK034) activation assay kits (Cytoskeleton, Denver, CO). [<sup>32</sup>P] LPA and [<sup>32</sup>P]sphingosine 1-phosphate (S1P) were prepared as described previously (17, 28) and diluted with nonradioactive substrate to a specific radioactivity of 1 × 10<sup>7</sup> cpm/μmol.

### Lentivirus generation and establishment of stable cell lines

GFP, FLAG-tagged mouse LPP1, and the catalytically inactive mutant LPP1(R217K) flanked by restriction enzyme sites *SpeI* and *SalI* were amplified by PCR and ligated into the entry vector pEN\_TTmcs (Addgene 25755) between enzyme sites *SpeI* and *XhoI*. The inserts were transferred into a lentiviral destination vector pSLIK-Neo (Addgene 25735) carrying a neomycin selection marker through LR recombination. Expression of inserts was controlled by a tetracycline-inducible promoter. Lentivirus was generated by cotransfecting the destination vector and packaging vectors: pMD2.G (Addgene 12259), pRSV-Rev (Addgene 12253), and pMDLg/pRRE (Addgene 12251) into HEK293T cells (ATCC, Manassas, VA). Culture medium containing lentivirus was collected on days 2 and 3 after transfection. Lentivirus was concentrated by ultracentrifugation at 40,000 rpm for 2 h (Beckman Type 50.2 Ti rotor) and resuspended in 0.5 ml DMEM. MDA-MB-231 (human) and 4T1 (mouse) mammary carcinoma cell lines were from ATCC. The 4T1-12B cell line was from Dr. Sahagian (Tufts University School of Medicine, MA). Human

thyroid carcinoma cell line TPC-1 was from Dr. S Ezzat (University of Toronto, Ontario, Canada). Cells were maintained in DMEM containing 10% FBS. Cells were transduced with lentiviruses and selected by G418 (1 mg/ml) for 7 days. Recombinant proteins were expressed by adding 1  $\mu$ g/ml doxycycline to induce the promoter.

### Assays for LPP1, LPA, phosphatidate, and diacylglycerol

Total LPP activity and the ecto-LPP activity against LPA were measured as described (17). SIP and LPA molecular species were measured in plasma and tumors by mass spectrometry (13). Phosphatidate and diacylglycerol were measured in cells after labeling for 2 h with 20  $\mu$ Ci of carrier-free [ $^3$ H]palmitate (21).

### Real-time PCR, Western blotting, and Immunohistochemistry

Expressions of LPPs and LPA<sub>1</sub> and LPA<sub>2</sub> receptors were determined by real-time RT-PCR (8). Western blotting and immunohistochemistry were performed as described previously (13).

### Intracellular Ca<sup>2+</sup>-mobilization assay

MDA-MB-231 cells were serum starved overnight and detached with PBS containing 2 mM EDTA and 0.1% (w/v) BSA, pH 7.4. Cells were washed and suspended in Ca<sup>2+</sup>, Mg<sup>2+</sup>, and phenol red-free Hank's buffer containing 2.5  $\mu$ M probenecid and 0.1% (w/v) BSA. Cells were labeled with 2 mM Fura-2 AM plus 0.02% (w/v) F127 and incubated in the dark at 20°C for 40 min. After washing, cells were suspended in the same buffer (5  $\times$  10<sup>5</sup> cells/ml), and 2 ml of cell suspension was loaded into a quartz cuvette for fluorescence measurement using a fluorometer (C43/2000, PTI). The ratio of emission intensity at 510 nm after 340 and 380 nm excitation was used to calculate Ca<sup>2+</sup> mobilization.

### Small GTPase activation assay

Cells were serum starved overnight and stimulated by agonists. Cells were lysed and GTP-bound RhoA, Cdc42, and Rac1 were pulled down by Rhotekin-RBD and PAK-PBD conjugated beads, respectively, using a commercial kit. The GTP-bound G-proteins were separated by 13% SDS-PAGE and detected by Western blotting using kit antibodies.

### Cell proliferation assay in monolayer and 3D culture

For monolayer culture, MDA-MB-231 cells were suspended in phenol red-free DMEM/10% FBS and seeded in 96-well plates (5,000 cells per well). Cell growth was monitored for 6 days. Optical density at 570 nm (OD<sub>570nm</sub>) was measured at each day after incubating for 1.5 h at 37°C with 1 mM 3-(4,5-dimethylthiazol-2-yl)-2,5-diphenyltetrazolium bromide (MTT) in the culture medium. For 3D culture, MDA-MB-231 cells were suspended in DMEM (1.5  $\times$  10<sup>4</sup> cells/ml) supplemented with 2% (v/v) growth factor-reduced Matrigel and 10% (v/v) FBS or charcoal-stripped FBS (FBSC). Cell suspension (400  $\mu$ l/well) was put onto the top of a thin layer of Matrigel (150  $\mu$ l/well) in 8-well chamber slides (177402; Thermo Scientific). Cells were grown for 8 days with daily replacement with fresh medium and fixed with 4% (w/v) paraformaldehyde. Phase-contrast images were taken (DM IRB, Leica), and the average size of cell colonies was measured by ImageJ software.

### Cell migration assay

MDA-MB-231 cells were serum starved overnight and detached with PBS containing 2 mM EDTA and 0.1% (w/v) BSA, pH 7.4. Cells were washed three times with serum-free DMEM and suspended in DMEM containing 0.1% (w/v) BSA (3  $\times$  10<sup>5</sup> cells/ml). The top chambers of a 96-well Boyden chamber (MBB96, Neuro

Probe) were loaded with 100  $\mu$ l of cell suspension, and the bottom chambers filled with DMEM and agonists. Chambers were separated with a polycarbonate membrane, which had 8  $\mu$ m pores and was coated with fibronectin (10  $\mu$ g/ml) overnight at 4°C. Cell migration was measured over 4 h at 37°C. Cells on the membrane were fixed with methanol. Cells on the top surface of the membrane were removed by wiping. Cells that migrated to the bottom surface of the membrane were stained with Coomassie blue and quantified with an Odyssey infrared imaging system (LI-COR Biosciences).

### Mouse tumor models

Some cancer cells were induced with doxycycline for 3 days to express specified proteins. Following trypsinization and washing, cells were suspended in phenol red-free DMEM/Matrigel (1:1, v/v). A syngeneic orthotopic mouse breast tumor model was established as before (13). In the xenograft models, MDA-MB-231 cells (1  $\times$  10<sup>6</sup>) were injected into mammary fat pads of Fox-Chase-SCID<sup>®</sup> beige (CB17.Cg-Prkdc<sup>scid</sup>Lys<sup>bg/l</sup>/Cr1) mice. TPC-1 cells (5  $\times$  10<sup>5</sup>) were injected subcutaneously into the flank. Expression of exogenous proteins was maintained by adding 2 mg/ml doxycycline to the drinking water. Tumor growth was monitored as before (13). To establish a metastatic model, 4T1 cells (1.5  $\times$  10<sup>5</sup>, in PBS) were injected into BALB/c mice through the tail vein. Lungs were fixed and stained with India ink and the number of nodules counted. Eight- to ten-week-old mice were from Charles River (Kingston, Ontario, Canada). All procedures complied with the Canadian Council of Animal Care as approved by the University of Alberta Animal Welfare Committee.

### Statistical analysis

Results were analyzed by two-tailed Student's *t*-test or one-way ANOVA with post hoc test for significance (*P* < 0.05).

## RESULTS

### Characterization of cancer cells that inducibly expressed LPP1, LPP1(R217K), or GFP

We studied the effects of LPP1 expression on cancer progression using aggressive triple negative mouse 4T1-12B and 4T1 mouse breast cancer cells, human MDA-MB-231 breast cancer cells, and human TPC-1 thyroid cancer cells. These cells were transduced with lentiviral vectors to create stable cell lines in which we could express GFP and FLAG-tagged LPP1 and its catalytically inactive mutant LPP1 (R217K) by induction with doxycycline (Fig. 1A–D).

Treatment of these cells with doxycycline increased the total expression of mRNA for LPP1 by about 5-fold in cells, whereas there were no significant effects on mRNA levels for LPP2 and LPP3 (supplementary Fig. IIA, B). Expression of LPP1 increased the mRNA for LPA<sub>1</sub> and LPA<sub>2</sub> receptors by about 1.5-fold in MDA-MB-231 cells, but the LPA<sub>1</sub> protein was not changed (supplementary Fig. IIC, D).

Expression of LPP1 in MDA-MB-231 and 4T1-12B cells increased total LPP activity (which included activities from LPP2 and LPP3) by about 2-fold, whereas LPP1 (R217K) had no significant effect (Fig. 1E, F). Overexpression of LPP1 in intact MDA-MB-231 cells increased the extracellular

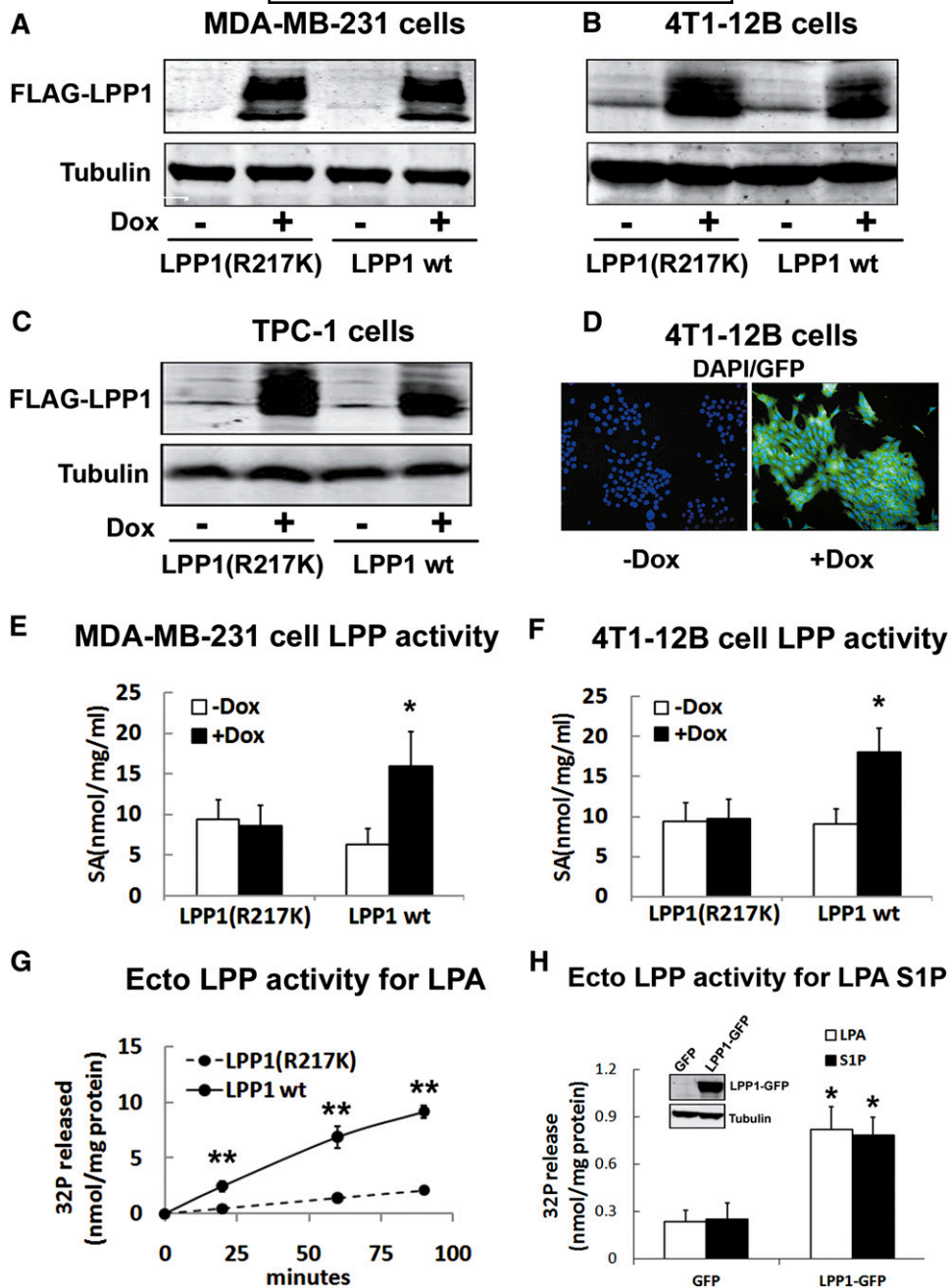


**Fig. 1.** Inducible expression of GFP, LPP1, and LPP1 (R217K) in cancer cells. LPP1 (LPP1 wt) and inactive LPP1 (R217K) were induced with 1  $\mu$ g/ml of doxycycline (Dox) for 3 days in MDA-MB-231 and 4T1-12B breast cancer cells (A, B) and in TPC-1 thyroid cancer cells (C). GFP expression was also induced in 4T1-12B cells (D,  $\times 200$  magnification). Total LPP activity in MDA-MB-231 (E) and 4T1-12B (F) cell lines is shown in induced and noninduced cells. Ecto-activity against [ $^{32}$ P]LPA (G) is shown for MDA-MB-231 that expressed LPP1 or LPP1 (R217K). H: The effect of overexpressing GFP-tagged LPP1 in HEK 293 cells is shown in the inset. Changes in ecto-phosphatase activity against LPA and SIP are shown. Results are means  $\pm$  SD from three independent experiments. Significant differences between cells expressing LPP1 or LPP1 (R217K) groups are shown as \*  $P < 0.05$  and \*\*  $P < 0.01$ .

dephosphorylation of [ $^{32}$ P]LPA by 5-fold compared with LPP1 (R217K) (Fig. 1G). This demonstrates that some recombinant LPP1 was located on the cell surface.

We also tested whether LPP1 can dephosphorylate extracellular SIP, which is a sphingolipid analog of LPA that activates five specific receptors to increase cell survival. To do this, we specifically induced a large (90-fold) overexpression

of total LPP1 activity in HEK 293 cells as measured in homogenates using phosphatidate as a substrate. This LPP1 was GFP-tagged at the C terminus, and it increased the degradation of extracellular SIP to the same extent as that observed with LPA (Fig. 1H). This demonstrates that LPP1 has similar ecto-phosphatase activity against LPA and SIP.

## Effects of expressing LPP1 on cell proliferation, cell migration, and signaling

We investigated whether increasing LPP1 expression in cancer cells could modify cell growth in monolayer culture but found no significant effect (results not shown). Cells cultured in 3D conditions form natural and more complex cell-cell and cell-extracellular matrix interactions, which are closer to those found in tissues (29). The average colony size of LPP1-overexpressing MDA-MB-231 cells cultured in 10% FBS was decreased by ~50% relative to the inactive LPP1(R217K) (Fig. 2A). Doxycycline (1  $\mu$ g/ml) itself appeared to inhibit cell growth slightly, but the effect was not statistically significant, and it was much

weaker than that of LPP1. When the cells were cultured in 10% FBSC to remove LPA (7), the average colony size of LPP1(R217K) cells decreased by ~50% relative to the cells cultured in 10% untreated FBS, and induction of LPP1 had no significant effect (Fig. 2B). Adding 5  $\mu$ M LPA back to FBSC partially restored the colony size of LPP1(R217K)-expressing cells but had no effect on cells expressing wild-type LPP1. Taken together, these results show that LPP1 expression decreases LPA-induced increase in colony size of MDA-MB-231 cells.

Doxycycline-induced expression of LPP1 also significantly inhibited LPA-stimulated migration of MDA-MB-231 cells. These cells express epidermal growth factor receptor-1,

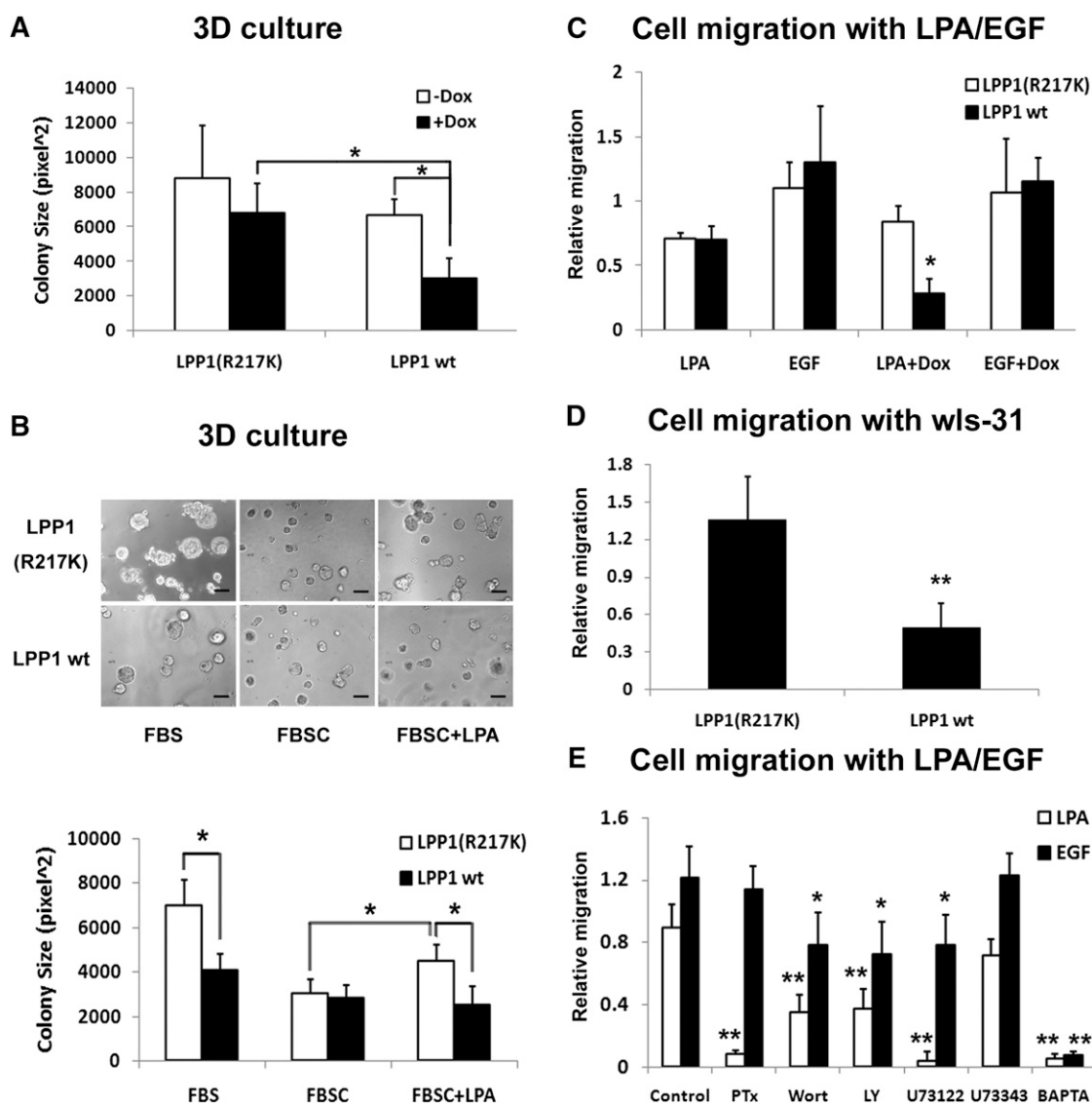


**Fig. 2.** Inhibitory effects of LPP1 on MDA-MB-231 cell growth and migration. A: Colony size of induced and noninduced MDA-MB-231 cells grown in 3D culture with 10% FBS. B: Representative phase contrast images (scale bar = 100  $\mu$ m) and colony size of doxycycline (Dox)-induced MDA-MB-231 cells in 3D culture with 10% FBS, 10% FBSC, and FBSC plus 5  $\mu$ M LPA. C: Migration of induced and noninduced MDA-MB-231 cells in response to LPA (0.5  $\mu$ M) or EGF (10 ng/ml). D: Migration of induced MDA-MB-231 cells in response to 1  $\mu$ M wls-31. E: Migration of normal MDA-MB-231 cells in response to LPA (0.5  $\mu$ M) or EGF (10 ng/ml) with or without pretreatment with inhibitors: 0.2  $\mu$ g/ml PTX for 16 h, 0.2  $\mu$ M wortmannin (wort) for 30 min, 10  $\mu$ M LY294002 (LY) for 30 min, 2  $\mu$ M U73122 for 30 min, 2  $\mu$ M U73343 for 30 min, 25  $\mu$ M BAPTA-AM for 30 min. Significant differences between LPP1 and LPP1(R217K) cells are shown as \*  $P < 0.05$  and \*\*  $P < 0.01$ . Results are means  $\pm$  SD from three independent experiments.

and LPP1 had no effect on EGF-induced migration (Fig. 2C). LPP1 also blocked cell migration that was stimulated with wls-31, an LPA<sub>1/2</sub> agonist (Fig. 2D) (27). Wls-31 is an  $\alpha$ -hydroxyphosphonate analog of LPA that cannot be dephosphorylated by LPP1. Therefore, this effect of LPP1 on migration cannot be explained by its ecto-activity.

LPA<sub>1</sub> and LPA<sub>2</sub> receptors couple to G<sub>i/o</sub>, G<sub>q</sub>, and G<sub>12/13</sub>. LPA-induced migration of MDA-MB-231 was completely blocked by PTX (Fig. 2E), showing the involvement of G<sub>i/o</sub>. The downstream effectors of G<sub>i/o</sub> include phosphoinositide 3-kinase (PI3K) and phospholipase C (PLC). In agreement with this, wortmannin and LY294002 (PI3K inhibitors), U73122 (a PLC inhibitor), and BAPTA-AM (a chelator of intracellular Ca<sup>2+</sup>) significantly blocked LPA-induced cell migration, whereas the inactive U73343 had no significant effect. As expected, PTX did not affect EGF-mediated migration, but there was an inhibition by blocking PI3K, PLC, and Ca<sup>2+</sup> signaling (Fig. 2E).

To determine how LPP1 could inhibit LPA-induced cell migration, we measured effects on Ca<sup>2+</sup> mobilization. LPP1 expression attenuated LPA-stimulated Ca<sup>2+</sup> transients in MDA-MB-231 cells compared with controls where LPP1 (R217K) was expressed or when the cells were not induced with doxycycline (Fig. 3A). LPP1 expression also attenuated the Ca<sup>2+</sup> transients produced by the nondephosphorylatable LPA analog, wls-31 (Fig. 3B). These results could be explained if LPP1 were to decrease Ca<sup>2+</sup> stores in the endoplasmic reticulum. This possibility was excluded because the thapsigargin-induced Ca<sup>2+</sup> accumulation was not significantly different in cells expressing LPP1 or LPP1 (R217K) (Fig. 3C).

LPA-induced Ca<sup>2+</sup> transients in MDA-MB-231 cells were completely blocked by PTX demonstrating G<sub>i/o</sub>-mediated signaling (Fig. 3D). We also used PARI peptide, an agonist of the PARI receptor, which couples to G<sub>i/o</sub>, G<sub>q</sub>, and G<sub>12/13</sub>. PARI-peptide-stimulated Ca<sup>2+</sup> transients were much less sensitive to PTX (Fig. 3D), showing that signaling was mainly mediated through a PTX-insensitive pathway, as reported elsewhere (30, 31). Interestingly, LPP1 potently blocked Ca<sup>2+</sup> transients induced by PARI peptide (Fig. 3E).

Both G<sub>i/o</sub> and G<sub>q</sub> activate PLC $\beta$  as a downstream effector to induce Ca<sup>2+</sup> release from the endoplasmic reticulum. LPP1 showed very similar potency in inhibiting both LPA- and PARI-stimulated Ca<sup>2+</sup> mobilization, which demonstrates that LPP1 attenuates signaling through PLC $\beta$ -Ca<sup>2+</sup> when activated by both G<sub>i/o</sub> and G<sub>q</sub>.

Activation of the Rho family of GTPases is mediated by G<sub>12/13</sub>, which plays a critical role in cytoskeleton dynamics and cell movement. LPP1 overexpression blocked LPA-stimulated increases in GTP-bound RhoA, but not GTP-bound Cdc42 and Rac1 (Fig. 4A, C). EGF-induced RhoA activation was not affected by LPP1 (Fig. 4B, C). These results are compatible with the LPP1 effects in attenuating LPA-stimulated, but not EGF-stimulated, cell migration (Fig. 2D). RhoA activation peaked within 5 min following stimulation with 1  $\mu$ M LPA.

LPA-induced Akt phosphorylation in MDA-MB-231 cells was inhibited by PTX (supplementary Fig. IIIA), but not by overexpressing LPP1 (supplementary Fig. IIB). This

shows that LPP1 does not affect the G<sub>i/o</sub>-PI3K-Akt pathway. LPA-induced ERK phosphorylation was also not affected by LPP1 (supplementary Fig. IIIB). We also did not observe effects of LPP1 on EGF-induced Akt and ERK phosphorylation (supplementary Fig. IIIC).

Increasing LPP1 expression in fibroblasts blocks phospholipase D (PLD) activation by LPA and platelet-derived growth factor (PDGF). PLD2 activation is required for LPA-induced fibroblast migration. This situation appears to be different in MDA-MB-231 cells because we were unable to block LPA-induced migration by inhibiting PLD with 1  $\mu$ M VU0155056, 0.5  $\mu$ M VU0359595, or 1  $\mu$ M VU0285655-1, or by diverting the PLD reaction to the formation of phosphatidylbutanol by adding 30 mM butan-1-ol. By contrast, PLD inhibition blocked the migration of Rat2 fibroblasts in the same experiment (results not shown). Expression of LPP1 did not attenuate PLD activation and the increased accumulation of phosphatidate or diacylglycerol in the MDA-MB-231 cells (supplementary Fig. IVA–C).

### Increased LPP1 in cancer cells inhibited tumor growth and metastasis

We next evaluated how these LPP1-induced changes in signaling affect the formation of tumors and metastases in mice using a syngeneic orthotopic model of breast cancer. Modified mouse 4T1-12B cells were pretreated with doxycycline for 3 days to induce expression of LPP1 or GFP, and these cells were injected into the right and left mammary fat pads, respectively, of the same mouse. Exogenous protein expression was sustained by adding doxycycline in the drinking water. The growth of tumors from 4T1-12B cells that overexpressed LPP1 was almost completely suppressed compared with tumors derived from GFP-expressing cells (Fig. 5A, B). As further controls, we studied tumor growth from the equivalent cells that were not induced with doxycycline, and there was no significant difference between the two cell lines (Fig. 5C, D). The inhibition of tumor growth by LPP1 relied on its phosphatase activity because increasing the expression of LPP1 (R217K) did not affect tumor growth (Fig. 5C, D). However, there was no significant effect of LPP1 expression in the cancer cells on concentrations of S1P or molecular species of LPA in the plasma or tumors of the mice (supplementary Fig. V).

We also determined the effects of inducing the expression of LPP1 at different times after the tumors were palpable. Tumor growth was essentially halted when doxycycline was added to the drinking water to induce LPP1 expression at days 6 and 8 after the injection of the noninduced cells (Fig. 5E).

Tumors derived from 4T1-12B cells expressing LPP1 showed a decrease in Ki67 (proliferation marker)-positive cells (Fig. 5F, G). The number of CD31-positive vascular endothelium cells averaged 55  $\pm$  42 and 74  $\pm$  32 per field for cells expressing LPP1 and LPP1 (R217K), respectively, but this is not significant different ( $P = 0.23$ ). However, the tumors produced by 4T1 cells are not particularly vascular, and further studies are needed to determine whether LPP1 expression in cancer cells changes angiogenesis in

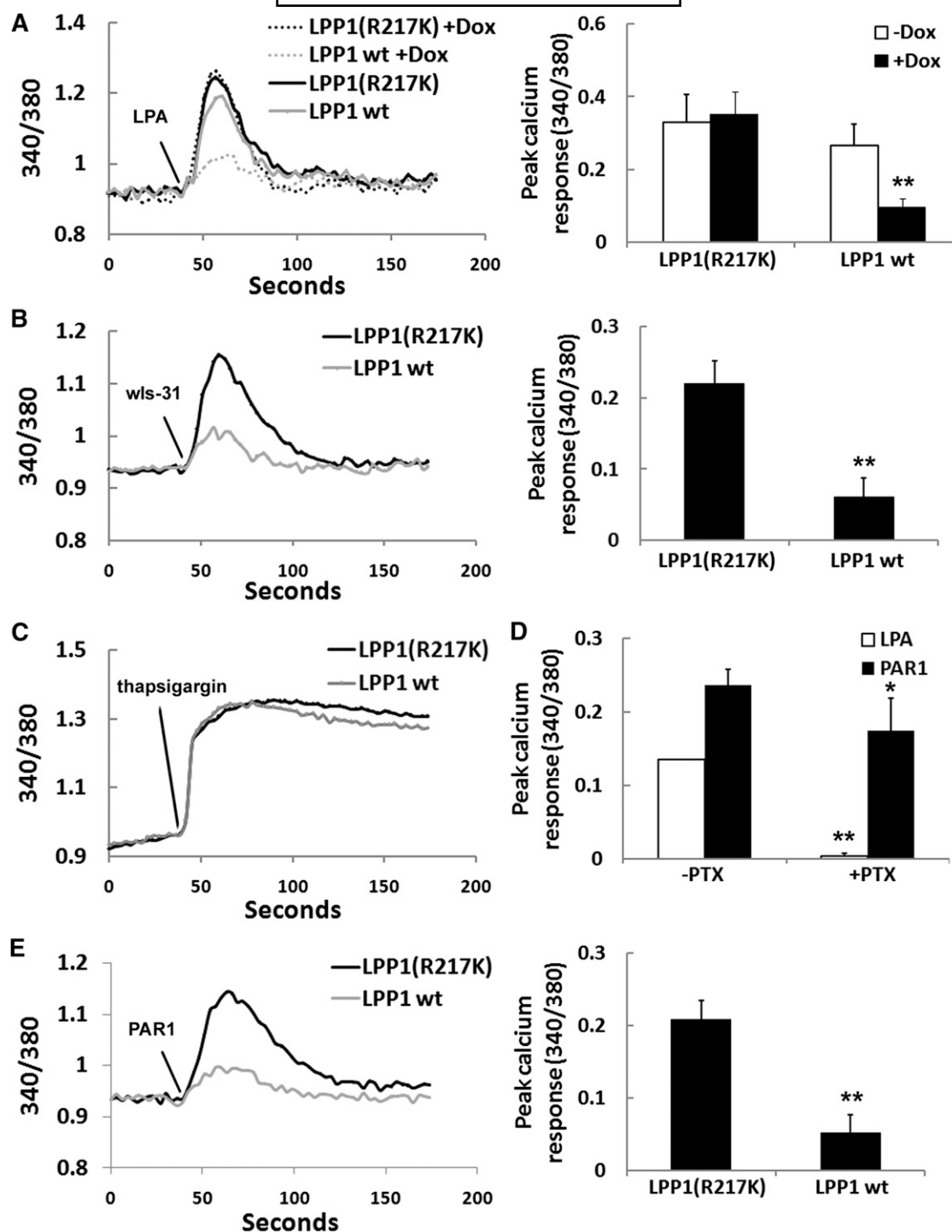


**Fig. 3.** LPP1 suppresses LPA- and PAR1-mediated  $\text{Ca}^{2+}$  mobilization. A: LPA (10  $\mu\text{M}$ ) stimulated  $\text{Ca}^{2+}$  mobilization in doxycycline (Dox)-induced and noninduced MDA-MB-231 cells. B: Wls-31 (20  $\mu\text{M}$ ) stimulated  $\text{Ca}^{2+}$  mobilization in induced MDA-MB-231 cells. C: Thapsigargin (1  $\mu\text{M}$ ) mediated  $\text{Ca}^{2+}$  mobilization in induced MDA-MB-231 cells. D: Effects of PTX on the stimulation of  $\text{Ca}^{2+}$  mobilization by 10  $\mu\text{M}$  LPA or 25  $\mu\text{M}$  PAR1 peptide in normal MDA-MB-231 cells. E: Effects of LPP1 on PAR1-peptide-mediated  $\text{Ca}^{2+}$  mobilization in induced MDA-MB-231 cells. Significant differences between LPP1 and LPP1(R217K) cells are shown as \*  $P < 0.05$  and \*\*  $P < 0.01$ . Results are means  $\pm$  SD from three independent experiments.

the tumor. The number of TUNEL-positive cells (Fig. 5F) and poly ADP-ribose polymerase cleavage (apoptotic markers) were not changed by LPP1 expression (results not shown). These findings demonstrate that the decreased tumor growth in cells expressing LPP1 was mediated mainly through inhibiting cell proliferation.

The inhibition of tumor growth by LPP1 was confirmed with two xenograft models using severe combined immunodeficient (SCID) mice. MDA-MB-231 cells overexpressing LPP1 were injected orthotopically into the mammary fat pad, and they formed smaller tumors relative to tumors from cells expressing LPP1(R217K) (Fig. 6A, B). We also

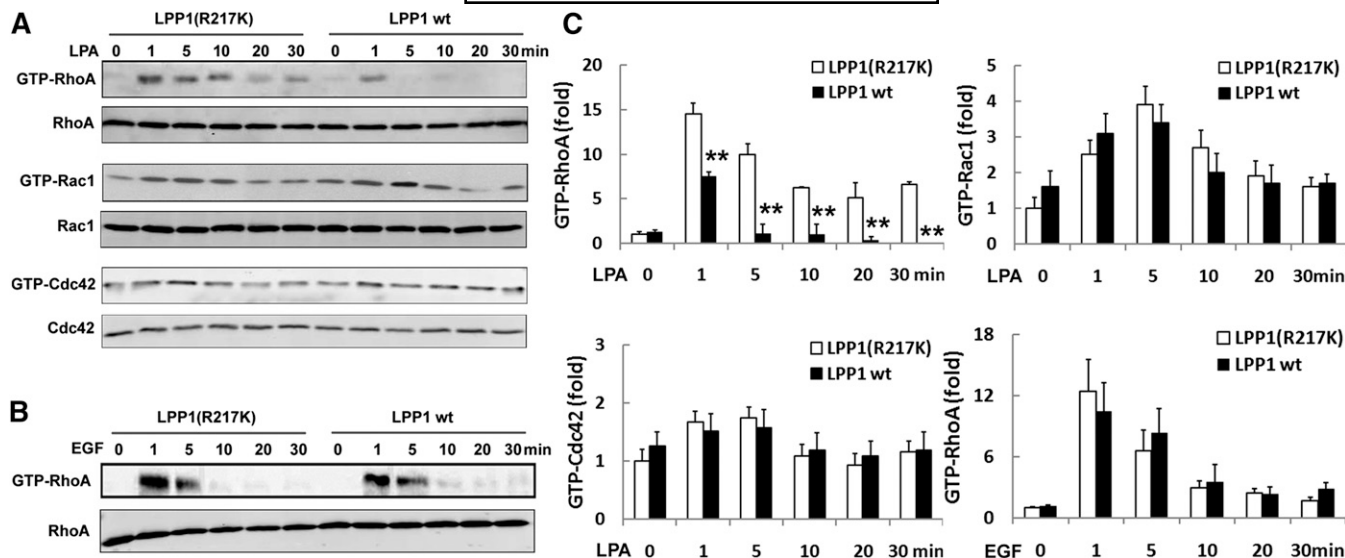


**Fig. 4.** LPP1 inhibits LPA-stimulated RhoA activation. **A:** Time course for the formation GTP-bound RhoA, Rac1, and Cdc42 in doxycycline (Dox)-induced MDA-MB-231 cells stimulated with LPA (1  $\mu$ M). **B:** Time course for the formation of GTP-bound RhoA in doxycycline-induced MDA-MB-231 cells stimulated with EGF (50 ng/ml). **C:** Quantification of LPA- and EGF-stimulated RhoA, Rac1, and Cdc42 activation. Significant differences between LPP1 and LPP1(R217K) cells are shown as \*\*  $P < 0.01$ . Results are means  $\pm$  SD from three independent experiments.

overexpressed LPP1 in human papillary thyroid cancer cells (TPC-1). These cells were injected into the flanks of SCID mice. Expression of LPP1 also significantly suppressed tumor growth compared with the LPP1(R217K) (Fig. 6C, D).

To examine whether LPP1 inhibits metastasis of breast cancer cells, we used mouse 4T1 breast cancer cells, which produce large numbers of lung metastases compared with 4T1-12B cells (32). Expression of LPP1 compared with LPP1(R217K) decreased the number of nodules in the lungs by  $\sim 80\%$  at day 29 after injection (Fig. 7A). At this very late stage, the average size of the corresponding primary tumor was  $\sim 40\%$  lower ( $P < 0.01$ ) compared with injecting LPP1(R217K)-expressing cells (results not shown).

The second experimental model involved tail vein injection of 4T1 cells into BALB/c mice to determine whether LPP1 decreases lung metastasis simply because of the slower growth of the primary tumor. Cells expressing LPP1 formed  $\sim 75\%$  fewer lung nodules compared with cells expressing LPP1(R217K) at day 14 after injection (Fig. 7B). Although this model bypasses some steps of metastasis, it still showed that the capability of the cancer cells for extravasation, survival, and growth at distant organs was decreased by LPP1. We also determined the number of lung micrometastasis in the xenograft model using MDA-MB-231 cells. The average colony number of metastatic cells in lung sections formed by expressing wild-type LPP1 in MDA-MB-231 cells was  $\sim 80\%$  less than that for the LPP1(R217K)-expressing cells (Fig. 7C).

## DISCUSSION

Extracellular LPA accumulation depends mainly on the balance of LPA production by ATX and degradation by

LPPs (2, 33). High ATX activity and LPA signaling in cancers promotes tumor growth, metastasis, and resistance to chemotherapy and radiotherapy (3, 34). It was predicted from work with cultured cells that this situation could be aggravated by low LPP1 expression in many cancer cells (2, 23, 25) and tumors (supplementary Fig. 1). The present studies are the first to test this hypothesis in animal models. Increasing the low LPP1 activity in very aggressive breast and thyroid cancer cells decreased their abilities to support tumor growth in mice. LPP1 expression also decreased metastasis using three experimental approaches. Catalytically inactive LPP1 had no significant effects, and this demonstrates the importance of LPP1 activity.

The LPPs are “ecto-phosphatases” (15, 17, 35), and LPP1 provides much of the capacity to dephosphorylate circulating LPA in vivo (18). Increased expression of LPP1 in cancer cells increased the degradation of exogenous LPA by 5-fold, which demonstrates that some recombinant LPP1 was expressed on the plasma membrane. We also demonstrated that LPP1 has the capacity to dephosphorylate extracellular S1P, which is also an important promoter of tumor progression and metastasis (36, 37).

However, overexpressing LPP1 in 4T1 cancer cells had no significant effect on the concentrations of S1P and different molecular species of LPA in plasma or breast tumors of the mice. This is not surprising because LPP1 was expressed only in the cancer cells, and the tumors also contain fibroblasts, endothelial cells, and leukocytes. Our previous work with an ATX inhibitor showed a substantial decrease in the concentrations of unsaturated LPA species in the breast tumors and plasma of mice in the same experimental model (13). This decrease in LPA should mimic the effects of a very substantial increase in ecto-LPA phosphatase activity. However, the antitumor effects of increased LPP1 expression are of greater magnitude

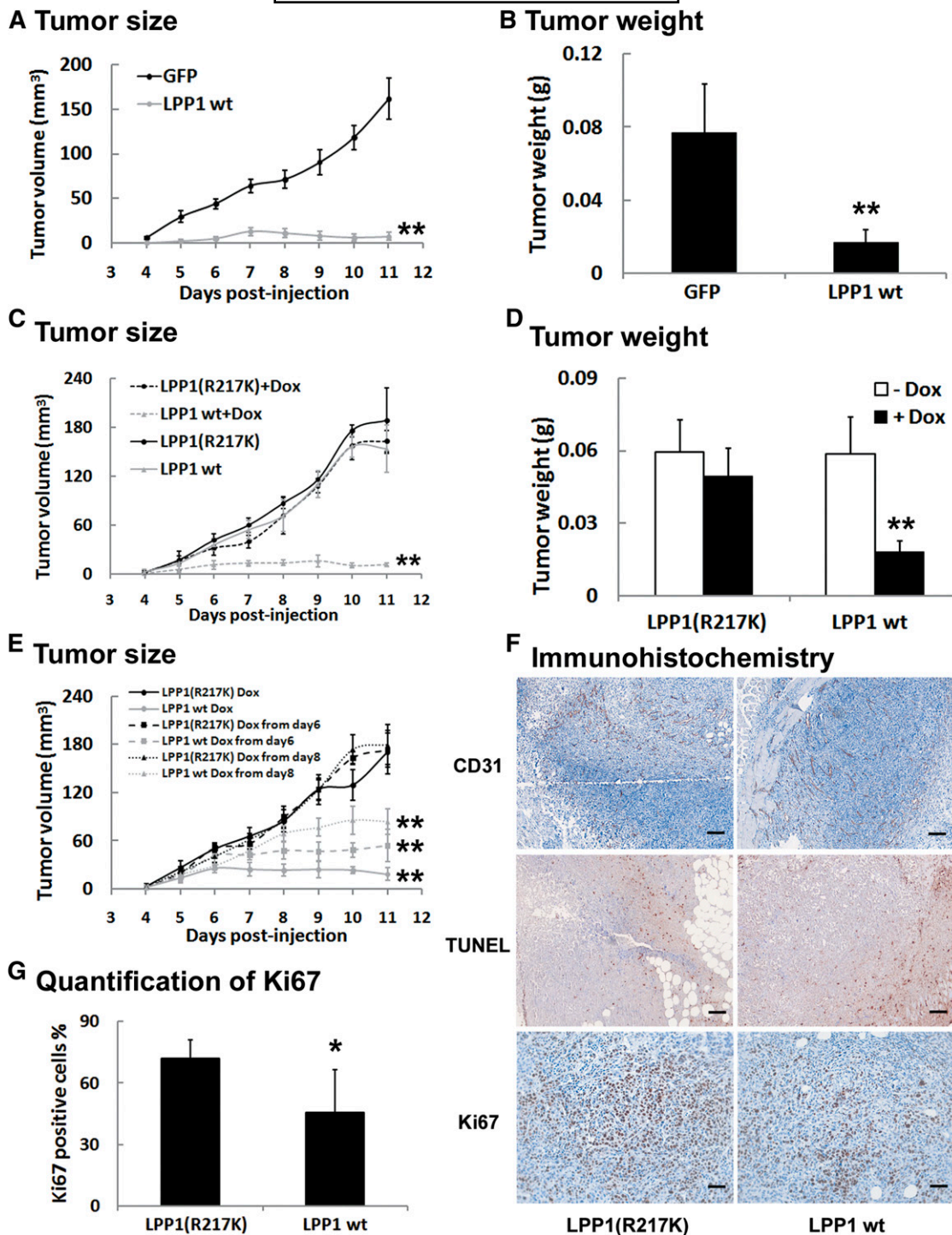


**Fig. 5.** LPP1 suppresses breast tumor growth in a mouse syngeneic orthotopic model. **A:** Tumor growth from doxycycline (Dox)-induced 4T1-12B cells transduced with LPP1 (LPP1 wt) or GFP in BALB/c mice ( $n = 5$  for each group). **B:** Weight of tumors from **A** on day 11 after implantation ( $n = 5$  for each group). **C:** Tumor growth from doxycycline-induced and noninduced 4T1-12B cells transduced with LPP1 or LPP1 (R217K) in BALB/c mice ( $n = 5$  for each group). **D:** Weight of tumors from **C** on day 11 after implantation ( $n = 5$  for each group). **E:** Tumor growth from 4T1-12B cells transduced with LPP1 or LPP1 (R217K) induced by doxycycline from 3 days before injection or induced by adding doxycycline to the drinking water on day 6 or 8 after implantation ( $n = 5$  for each group). **F:** Representative images of immunohistochemistry of tumor tissues from 4T1-12B cells expressing LPP1 and LPP1 (R217K); scale bar = 100  $\mu\text{m}$ . These were quantified by examining five different fields from each tumor and by using five mice per group. **G:** Quantification of average number of Ki67-positive tumor cells. Results are means  $\pm$  SD, and significant differences between LPP1 and LPP1 (R217K) groups are shown as \*  $P < 0.05$  and \*\*  $P < 0.01$ .

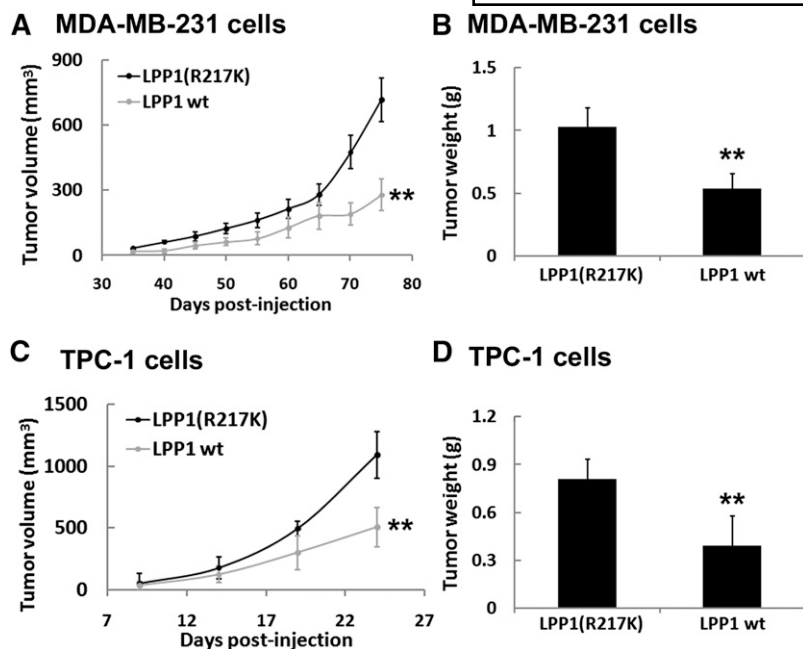


**Fig. 6.** LPP1 suppresses breast and thyroid tumor growth in mouse xenograft models. **A:** Tumor growth from MDA-MB-231 cells expressing wild-type LPP1 (LPP1 wt) or LPP1 (R217K) in SCID mice ( $n = 5$  for each group). **B:** Weight of tumors from **A** on day 75 after implantation ( $n = 5$  for each group). **C:** Tumor growth from TPC-1 cells expressing LPP1 or LPP1 (R217K) in SCID mice ( $n = 5$  for each group). **D:** Weight of tumors from **C** on day 24 after implantation ( $n = 5$  for each group). Results are means  $\pm$  SD, and significant differences between LPP1 and LPP1 (R217K) groups are shown as  $** P < 0.01$ .

and duration than those seen with ATX inhibition (13). Taken together, these results indicate that a major effect of LPP1 expression on tumor growth and metastasis depends on the attenuation of signaling downstream of G-protein-coupled receptors as predicted from cell culture experiments (2, 15, 38). We also demonstrated this effect in the present work because overexpression of LPP1 attenuates  $\text{Ca}^{2+}$  transients produced by PAR1 peptide, LPA, and the nondephosphorylatable LPA analog wls-31. Furthermore, LPP1 attenuated the  $\text{Ca}^{2+}$  transient generated by 1  $\mu\text{M}$  LPA within 1 min, and this cannot be explained by a significant change in LPA concentrations. This LPP1 effect depended on the catalytic activity of LPP1 as in other studies (21), but it cannot be explained by the ecto-LPP1 activity alone. We propose that LPP1 dephosphorylates an unidentified lipid phosphate that is required for transmitting the signal from activated receptors.

Increasing LPP1 expression decreased LPA-stimulated growth of breast cancer cells in 3D culture. This is compatible with the effect of LPP1 in decreasing the division of cancer cells in the breast tumors. It is not clear how LPP1 does this because there was no significant effect on the activations of ERK or Akt by either LPA or EGF.

The effect of LPP1 in decreasing the migration of MDA-MB-231 cells in response to LPA and wls-31 depended on decreased activation of PLC $\beta$  and  $\text{Ca}^{2+}$  mobilization. LPP1 expression also attenuates LPA-induced  $\text{Ca}^{2+}$  transients in Rat2 fibroblasts (17). This effect together with the decrease in LPA-induced activation of RhoA contributes to the attenuation of LPA-induced cancer cell migration and metastasis. There was no significant effect of LPP1 expression on EGF-stimulated migration of MDA-MB-231, which resembles the lack of effect of LPP1 on PDGF-induced migration in Rat2 fibroblasts (21). This latter work showed that LPP1 expression blocks the activation of PLD by both LPA and PDGF. However, the migration of fibroblasts requires phospholipase D2 activation, whereas activation

by PDGF does not. This situation appears to be different in MDA-MB-231 cells because we could not block LPA-induced migration by inhibiting PLD, whereas PLD inhibition blocked the migration of Rat2 fibroblasts in the same experiment (results not shown). Furthermore, expression of LPP1 in MDA-MB-231 cells did not attenuate PLD activation and the consequent LPA-induced increases in phosphatidate or diacylglycerol concentrations. Phosphatidate conversion to diacylglycerol in the PLD pathway is now thought to be catalyzed by a family of lipins rather than by LPPs (14).

The present studies establish that increasing the low LPP1 activity in breast cancer cells decreases LPA-dependent activation of  $\text{Ca}^{2+}$  transients and RhoA. This is accompanied by a decrease in LPA-induced stimulation of cell division and migration. This adds to the body of knowledge that has been assembled using cultured cells to define the signaling properties of LPP1. However, the major contribution of our present work is to translate this knowledge to the effects of increasing LPP1 expression in cancer cells in vivo. We demonstrate for the first time that increasing the low LPP1 expression in mouse and human breast cancer cells and in human thyroid cancer cells produced a profound and sustained decrease tumor growth and metastasis. This work with various mouse models provides “proof of principle” that targeting the ATX-LPA-LPP axis in cancer cells by increasing LPP1 expression could provide a novel strategy for treating breast and thyroid cancers. It is difficult to increase enzyme activities through therapeutic methods, but this is not impossible. For example, gonadotropin-releasing hormone increases ecto-LPP expression, and this decreases the proliferation of ovarian cancer cells (24). In the case of LPP1, we need to understand more about how its expression is regulated in cancer cells to be able to increase its activity. Alternatively, a therapeutic benefit could be gained by blocking key

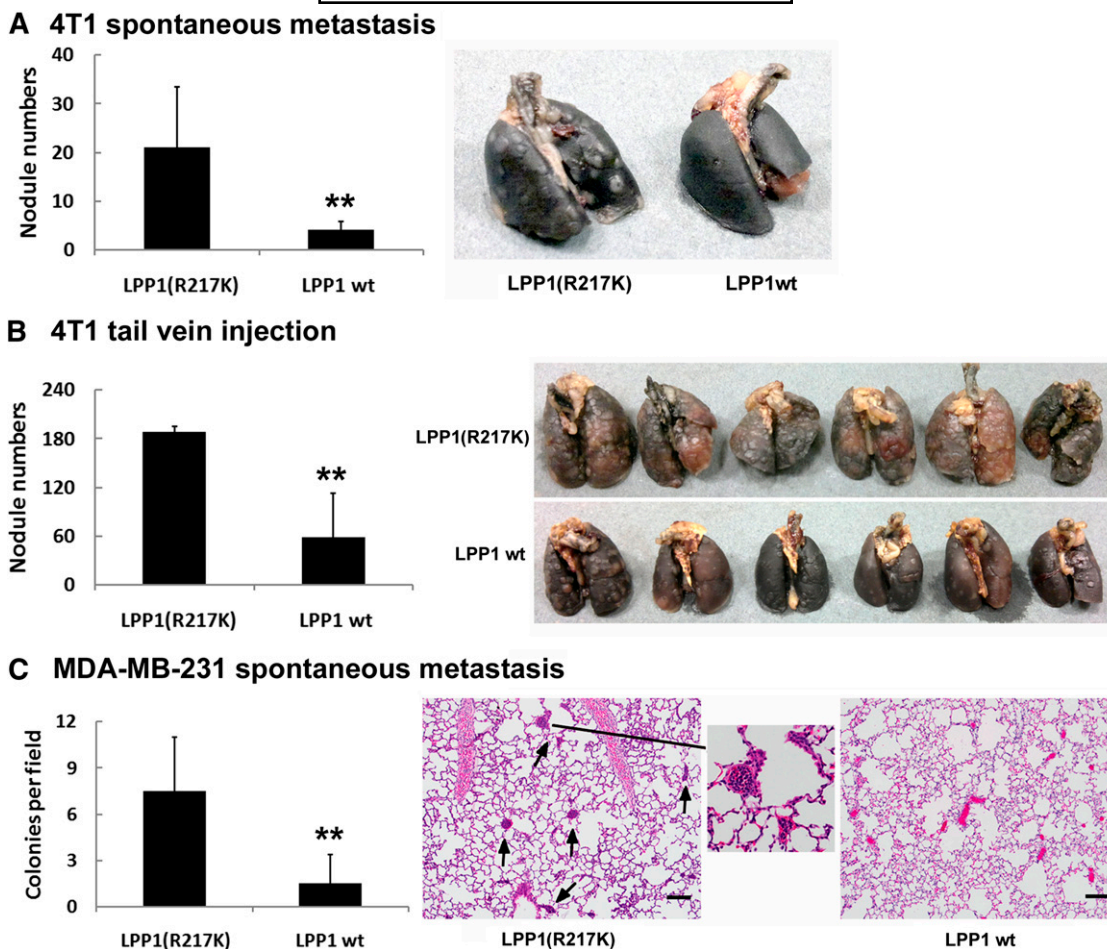


**Fig. 7.** LPP1 expression decreases lung metastasis. **A:** Number of lung nodules formed by 4T1 cells expressing LPP1 (LPP1 wt) or LPP1(R217K) in BALB/c mice on day 29 after orthotopic implantation ( $n = 6$  for each group). Right panel shows the representative lungs. **B:** Number of lung nodules formed by 4T1 cells expressing LPP1 or LPP1(R217K) in BALB/c mice on day 14 after tail vein injection ( $n = 6$  for each group). **C:** Average colony numbers of MDA-MB-231 cell expressing wild-type LPP1 or LPP1(R217K) in lung sections of SCID mice on day 75 after orthotopic implantation ( $n = 5$  for each group). Right panel shows the representative hematoxylin/eosin stained sections; scale bar = 100  $\mu\text{m}$ . Colonies of micrometastasis are indicated by arrows, and a representative magnified area is shown. Results are means  $\pm$  SD, and significant differences between LPP1 and LPP1(R217K) groups are shown as \*\* $P < 0.01$ .

signaling pathways that are also inhibited by increased LPP1 expression. **Fig. 7**

The authors thank Dr. M. Hollenberg for providing the PAR1 peptide and Dr. Marek Michalak for help and advice in measuring  $\text{Ca}^{2+}$  transients.

## REFERENCES

- Boutin, J. A., and G. Ferry. 2009. Autotaxin. *Cell. Mol. Life Sci.* **66**: 3009–3021.
- Samadi, N., R. Bekele, D. Capatos, G. Venkatraman, M. Sariahmetoglu, and D. N. Brindley. 2011. Regulation of lysophosphatidate signaling by autotaxin and lipid phosphate phosphatases with respect to tumor progression, angiogenesis, metastasis and chemo-resistance. *Biochimie.* **93**: 61–70.
- Benesch, M. G., Y. M. Ko, T. P. McMullen, and D. N. Brindley. 2014. Autotaxin in the crosshairs: taking aim at cancer and other inflammatory conditions. *FEBS Lett.* **588**: 2712–2727.
- Euer, N., M. Schwirzke, V. Evtimova, H. Burtscher, M. Jarsch, D. Tarin, and U. H. Weidle. 2002. Identification of genes associated with metastasis of mammary carcinoma in metastatic versus non-metastatic cell lines. *Anticancer Res.* **22**: 733–740.
- Liu, S., M. Umezū-Goto, M. Murph, Y. Lu, W. Liu, F. Zhang, S. Yu, L. C. Stephens, X. Cui, G. Murrow, et al. 2009. Expression of autotaxin and lysophosphatidic acid receptors increases mammary tumorigenesis, invasion, and metastases. *Cancer Cell.* **15**: 539–550.
- Popnikolov, N. K., B. H. Dalwadi, J. D. Thomas, G. J. Johannes, and W. T. Imagawa. 2012. Association of autotaxin and lysophosphatidic acid receptor 3 with aggressiveness of human breast carcinoma. *Tumour Biol.* **33**: 2237–2243.
- Samadi, N., C. Gaetano, I. S. Goping, and D. N. Brindley. 2009. Autotaxin protects MCF-7 breast cancer and MDA-MB-435 melanoma cells against Taxol-induced apoptosis. *Oncogene.* **28**: 1028–1039.
- Samadi, N., R. T. Bekele, I. S. Goping, L. M. Schang, and D. N. Brindley. 2011. Lysophosphatidate induces chemo-resistance by releasing breast cancer cells from taxol-induced mitotic arrest. *PLoS ONE.* **6**: e20608.
- Zhang, R., J. Wang, S. Ma, Z. Huang, and G. Zhang. 2011. Requirement of Osteopontin in migration and the protection against Taxol-induced apoptosis via ATX-LPA axis in SGC7901 cells. *BMC Cell Biol.* **12**: 11.
- Vidot, S., J. Witham, R. Agarwal, S. Greenhough, H. S. Bamrah, G. J. Tigyi, S. B. Kaye, and A. Richardson. 2010. Autotaxin delays apoptosis induced by carboplatin in ovarian cancer cells. *Cell. Signal.* **22**: 926–935.
- Bekele, R., and D. N. Brindley. 2012. Role of autotaxin and lysophosphatidate in cancer progression and resistance to chemotherapy and radiotherapy. *Clin. Lipidol.* **7**: 313–328.

12. Deng, W., E. Shuyu, R. Tsukahara, W. J. Valentine, G. Durgam, V. Gududuru, L. Balazs, V. Manickam, M. Arsura, L. VanMiddlesworth, et al. 2007. The lysophosphatidic acid type 2 receptor is required for protection against radiation-induced intestinal injury. *Gastroenterology*. **132**: 1834–1851.
13. Benesch, M. G., X. Tang, T. Maeda, A. Ohhata, Y. Y. Zhao, B. P. Kok, J. Dewald, M. Hitt, J. M. Curtis, T. P. McMullen, et al. 2014. Inhibition of autotaxin delays breast tumor growth and lung metastasis in mice. *FASEB J*. **28**: 2655–2666.
14. Kok, B. P., G. Venkatraman, D. Capatos, and D. N. Brindley. 2012. Unlike two peas in a pod: lipid phosphate phosphatases and phosphatidate phosphatases. *Chem. Rev.* **112**: 5121–5146.
15. Brindley, D. N., and C. Pilquill. 2009. Lipid phosphate phosphatases and signaling. *J. Lipid Res.* **50** (Suppl.): S225–S230.
16. Sigal, Y. J., M. I. McDermott, and A. J. Morris. 2005. Integral membrane lipid phosphatases/phosphotransferases: common structure and diverse functions. *Biochem. J.* **387**: 281–293.
17. Jasinska, R., Q. X. Zhang, C. Pilquill, I. Singh, J. Xu, J. Dewald, D. A. Dillon, L. G. Berthiaume, G. M. Carman, D. W. Waggoner, et al. 1999. Lipid phosphate phosphohydrolase-1 degrades exogenous glycerolipid and sphingolipid phosphate esters. *Biochem. J.* **340**: 677–686.
18. Tomsig, J. L., A. H. Snyder, E. V. Berdyshev, A. Skobeleva, C. Mataya, V. Natarajan, D. N. Brindley, and K. R. Lynch. 2009. Lipid phosphate phosphohydrolase type 1 (LPP1) degrades extracellular lysophosphatidic acid in vivo. *Biochem. J.* **419**: 611–618.
19. Yue, J., K. Yokoyama, L. Balazs, D. L. Baker, D. Smalley, C. Pilquill, D. N. Brindley, and G. Tigyi. 2004. Mice with transgenic overexpression of lipid phosphate phosphatase-1 display multiple organotypic deficits without alteration in circulating lysophosphatidate level. *Cell. Signal.* **16**: 385–399.
20. Alderton, F., P. Darroch, B. Sambhi, A. McKie, I. S. Ahmed, N. Pyne, and S. Pyne. 2001. G-protein-coupled receptor stimulation of the p42/p44 mitogen-activated protein kinase pathway is attenuated by lipid phosphate phosphatases 1, 1a, and 2 in human embryonic kidney 293 cells. *J. Biol. Chem.* **276**: 13452–13460.
21. Pilquill, C., J. Dewald, A. Cherney, I. Gorshkova, G. Tigyi, D. English, V. Natarajan, and D. N. Brindley. 2006. Lipid phosphate phosphatase-1 regulates lysophosphatidate-induced fibroblast migration by controlling phospholipase D2-dependent phosphatidate generation. *J. Biol. Chem.* **281**: 38418–38429.
22. Ile, K. E., R. Tripathy, V. Goldfinger, and A. D. Renault. 2012. Wunen, a Drosophila lipid phosphate phosphatase, is required for septate junction-mediated barrier function. *Development*. **139**: 2535–2546.
23. Martin, A., A. Gomez-Munoz, D. W. Waggoner, J. C. Stone, and D. N. Brindley. 1993. Decreased activities of phosphatidate phosphohydrolase and phospholipase D in ras and tyrosine kinase (fps) transformed fibroblasts. *J. Biol. Chem.* **268**: 23924–23932.
24. Imai, A., T. Furui, T. Tamaya, and G. B. Mills. 2000. A gonadotropin-releasing hormone-responsive phosphatase hydrolyses lysophosphatidic acid within the plasma membrane of ovarian cancer cells. *J. Clin. Endocrinol. Metab.* **85**: 3370–3375.
25. Tanyi, J. L., Y. Hasegawa, R. Lapushin, A. J. Morris, J. K. Wolf, A. Berchuck, K. Lu, D. I. Smith, K. Kalli, L. C. Hartmann, et al. 2003. Role of decreased levels of lipid phosphate phosphatase-1 in accumulation of lysophosphatidic acid in ovarian cancer. *Clin. Cancer Res.* **9**: 3534–3545.
26. Boucharaba, A., C. M. Serre, J. Guglielmi, J. C. Bordet, P. Clezardin, and O. Peyruchaud. 2006. The type 1 lysophosphatidic acid receptor is a target for therapy in bone metastases. *Proc. Natl. Acad. Sci. USA*. **103**: 9643–9648.
27. Hooks, S. B., W. L. Santos, D. S. Im, C. E. Heise, T. L. Macdonald, and K. R. Lynch. 2001. Lysophosphatidic acid-induced mitogenesis is regulated by lipid phosphate phosphatases and is Edg-receptor independent. *J. Biol. Chem.* **276**: 4611–4621.
28. Brindley, D. N., J. Xu, R. Jasinska, and D. W. Waggoner. 2000. Analysis of ceramide 1-phosphate and sphingosine-1-phosphate phosphatase activities. *Methods Enzymol.* **311**: 233–244.
29. Tang, X. J., Y. H. Fu, Q. H. Meng, L. M. Li, X. Y. Ying, M. Han, Q. J. He, B. Yang, S. Zeng, Y. Z. Hu, et al. 2013. Evaluation of pluronic nanosuspensions loading a novel insoluble anticancer drug both in vitro and in vivo. *Int. J. Pharm.* **456**: 243–250.
30. Sabri, A., J. Short, J. Guo, and S. F. Steinberg. 2002. Protease-activated receptor-1-mediated DNA synthesis in cardiac fibroblast is via epidermal growth factor receptor transactivation: distinct PAR-1 signaling pathways in cardiac fibroblasts and cardiomyocytes. *Circ. Res.* **91**: 532–539.
31. Tang, X., Z. Sun, C. Runne, J. Madsen, F. Domann, M. Henry, F. Lin, and S. Chen. 2011. A critical role of Gbetagamma in tumorigenesis and metastasis of breast cancer. *J. Biol. Chem.* **286**: 13244–13254.
32. Bahrami, F., D. L. Morris, and M. H. Pourgholami. 2012. Tetracyclines: drugs with huge therapeutic potential. *Mini Rev. Med. Chem.* **12**: 44–52.
33. Smyth, S. S., P. Mueller, F. Yang, J. A. Brandon, and A. J. Morris. 2014. Arguing the case for the autotaxin-lysophosphatidic acid-lipid phosphate phosphatase 3-signaling nexus in the development and complications of atherosclerosis. *Arterioscler. Thromb. Vasc. Biol.* **34**: 479–486.
34. Brindley, D. N., F. T. Lin, and G. J. Tigyi. 2013. Role of the autotaxin-lysophosphatidate axis in cancer resistance to chemotherapy and radiotherapy. *Biochim. Biophys. Acta.* **1831**: 74–85.
35. Zhang, Q. X., C. S. Pilquill, J. Dewald, L. G. Berthiaume, and D. N. Brindley. 2000. Identification of structurally important domains of lipid phosphate phosphatase-1: implications for its sites of action. *Biochem. J.* **345**: 181–184.
36. Pyne, N. J., and S. Pyne. 2010. Sphingosine 1-phosphate and cancer. *Nat. Rev. Cancer.* **10**: 489–503.
37. Shida, D., K. Takabe, D. Kapitonov, S. Milstien, and S. Spiegel. 2008. Targeting SphK1 as a new strategy against cancer. *Curr. Drug Targets.* **9**: 662–673.
38. Brindley, D. N. 2004. Lipid phosphate phosphatases and related proteins: signaling functions in development, cell division, and cancer. *J. Cell. Biochem.* **92**: 900–912.